

LYAPUNOV ORBITS AT L_2 AND TRANSVERSAL INTERSECTIONS OF INVARIANT MANIFOLDS IN THE JUPITER-SUN PLANAR RESTRICTED CIRCULAR THREE BODY PROBLEM

MACIEJ J. CAPIŃSKI *

Abstract. We present a computer assisted proof of existence of a family of Lyapunov orbits which stretches from L_2 up to half the distance to the smaller primary in the Jupiter-Sun planar restricted circular three body problem. We then focus on a small family of Lyapunov orbits with energies close to comet Oterma and show that their associated invariant manifolds intersect transversally. Our computer assisted proof provides explicit bounds on the location and on the angle of intersection.

Key words. Invariant manifolds, restricted three body problem, cone conditions, parameterization method, computer assisted proofs

AMS subject classifications. 37D10, 37N05, 34C20, 34C45, 70F07, 70F15

1. Introduction. The Planar Restricted Circular Three Body Problem (PRC-3BP) has been extensively studied throughout literature. The model has applications in space mission design [11, 12], explains symbolic dynamics phenomena observed in trajectories of comets [15] and can be used for study of diffusion estimates [13, 14]. All the above mentioned are associated with dynamics along invariant manifolds of the system. In this paper we discuss how existence of such manifolds can be proved within explicit bounds using rigorous-computer-assisted techniques.

We focus on dynamics associated with the fixed point L_2 , its associated center manifold and stable/unstable manifolds. The problem has been studied by Llibre, Martinez and Simo [16] where under appropriate conditions on parameters of the system existence and intersections of such manifolds has been proved analytically. In the work of Koon, Lo, Marsden and Ross [15] such invariant manifolds and their associated symbolic dynamics have been used to numerically explain a peculiar trajectory of the comet Oterma in the vicinity of Jupiter. Such symbolic dynamics has later been proved using rigorous-computer-assisted computations by Wilczak and Zgliczyński [19, 20]. The work presented in this paper can be viewed as an extension of last-mentioned. Results [19, 20] were obtained using purely topological arguments. They focus on homoclinic and heteroclinic tangle between periodic orbits, without the detection of the manifolds themselves or angles of their intersections. Here we address these issues.

In this paper we shall first present a method for detecting of families of Lyapunov orbits in the PRC3BP. It is designed as a tool for rigorous-computer-assisted proofs. We apply the method to obtain a family that spans up to half a distance between the fixed point L_2 and the smaller primary in the Jupiter-Sun system. This is our first main result, which is stated in Theorem 3.2. The method is based on a combination of interval Newton method and implicit function theorem.

We then consider a small family of Lyapunov orbits with energies close to the energy of comet Oterma. We prove that the family is normally hyperbolic, and give a tool for obtaining rigorous bounds for its unstable and stable fibers. The tool is based on a topological approach combined with a parameterization method. We then show

*The work was initiated during a visit of the author to University of Texas at Austin, sponsored by the Kościuszko Foundation. The work has been supported by the Polish State Ministry of Science and Information Technology grant N201 543238.

how fibers can be propagated to prove transversal intersections between stable and unstable manifolds of Lyapunov orbits. We investigate an intersection associated with manifolds which span from the Lyapunov orbit and circle around the larger primary. We obtain explicit bounds on the location of intersection and also on its angle. This is the second main result of the paper, which is stated in Theorem 4.1.

Both methods which we propose are tailor made for the PRC3BP. We make use of the preservation of energy and reversibility of the system. Thanks to this our rigorous bounds for the investigated manifolds are quite sharp.

For our method we also develop a more general tool which can be applied for the detection of unstable/stable manifolds of saddle - center fixed points. It is a generalization of the work of Zgliczyński [21]. This is the subject of section 6.

The paper is organized as follows. Section 2 includes preliminaries which give an introduction to the PRC3BP, the interval Newton method, and introduce some notations. In section 3 we present a method for detection of families of Lyapunov orbits and apply it to the Jupiter-Sun system. In section 4 we outline the results for the intersections of invariant manifolds, which are then proved throughout the remainder of the paper. In section 5 we show how to prove that Lyapunov orbits are hyperbolic and foliated by energy. In section 6 we give a topological tool for detection of unstable manifolds of saddle-center fixed points. The method is then combined with parametrization method in section 7 to obtain rigorous bounds on the intersections of invariant manifolds. Sections 8, 9 and 10 contain respectively closing remarks, acknowledgements and the appendix.

2. Preliminaries.

2.1. The Planar Restricted Circular Three Body Problem. In the Planar restricted circular three body problem (PRC3BP) we consider the motion of a small massless particle under the gravitational pull of two larger bodies (which we shall refer to as primaries) of mass μ and $1 - \mu$. The primaries move around the origin on circular orbits of period 2π on the same plane as the massless body. In this paper we shall consider the mass parameter $\mu = 0.0009537$, which corresponds to the rescaled mass of Jupiter in the Jupiter-Sun system.

The Hamiltonian of the problem is given by [1]

$$H(q, p, t) = \frac{p_1^2 + p_2^2}{2} - \frac{1 - \mu}{r_1(t)} - \frac{\mu}{r_2(t)},$$

where $(p, q) = (q_1, q_2, p_1, p_2)$ are the coordinates of the massless particle and $r_1(t)$ and $r_2(t)$ are the distances from the masses $1 - \mu$ and μ respectively.

After introducing a new coordinates system (x, y, p_x, p_y)

$$\begin{aligned} x &= q_1 \cos t + q_2 \sin t, & p_x &= p_1 \cos t + p_2 \sin t, \\ y &= -q_1 \sin t + q_2 \cos t, & p_y &= -p_1 \sin t + p_2 \cos t, \end{aligned} \quad (2.1)$$

which rotates together with the primaries, the primaries become motionless (see Figure 2.1) and one obtains [1] an autonomous Hamiltonian

$$H(x, y, p_x, p_y) = \frac{(p_x + y)^2 + (p_y - x)^2}{2} - \Omega(x, y), \quad (2.2)$$

where

$$\Omega(x, y) = \frac{x^2 + y^2}{2} + \frac{1 - \mu}{r_1} + \frac{\mu}{r_2},$$

$$r_1 = \sqrt{(x - \mu)^2 + y^2}, \quad r_2 = \sqrt{(x + 1 - \mu)^2 + y^2}.$$

The motion of the particle is given by

$$\dot{q} = J\nabla H(q), \quad (2.3)$$

where $q = (x, y, p_x, p_y) \in \mathbb{R}^4$, $J = \begin{pmatrix} 0 & \text{id} \\ -\text{id} & 0 \end{pmatrix}$ and id is a two dimensional identity matrix.

The movement of the flow (2.3) is restricted to the hypersurfaces determined by the energy level h ,

$$M(h) = \{(x, y, p_x, p_y) \in \mathbb{R}^4 | H(x, y, p_x, p_y) = h\}. \quad (2.4)$$

This means that movement in the x, y coordinates is restricted to the so called Hill's region defined by

$$R(h) = \{(x, y) \in \mathbb{R}^2 | \Omega(x, y) \geq -h\}.$$

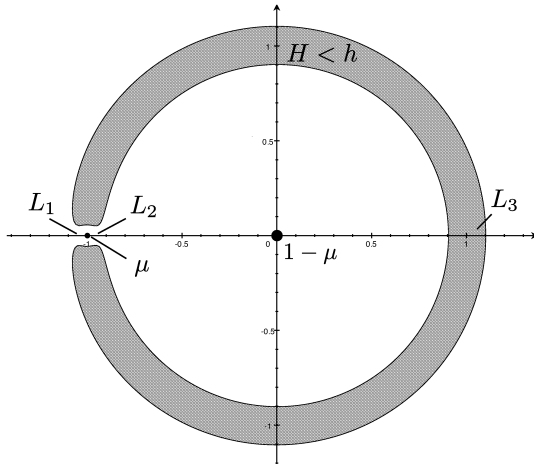


FIG. 2.1. The Hill's region for the energy level $h = 1.515$ of comet Oterma in the Jupiter-Sun system.

The problem has three equilibrium points L_1, L_2, L_3 on the x -axes (see Figure 2.1). We shall be interested in the dynamics associated with L_2 , and with orbits of energies higher than that of L_2 . The linearized vector field at the point L_2 has two real and two purely imaginary eigenvalues, thus by the Lyapunov theorem (see for example [16]) for energies h larger and sufficiently close to $H(L_2)$ there exists a family of periodic orbits parameterized by energy emanating from the equilibrium point L_2 . Numerical evidence shows that this family extends up to and even beyond the smaller primary μ [3].

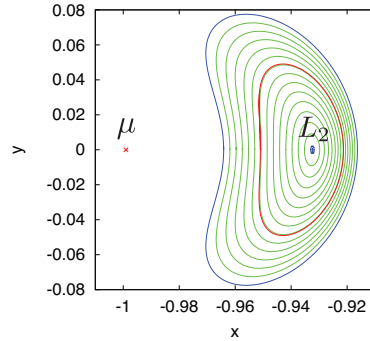


FIG. 2.2. Considered by us family of Lyapunov orbits in green (spanning between two orbits in blue), together with the Lyapunov orbit for the energy of the comet Oterma $h = 1.515$ in red.

The PRC3BP admits the following reversing symmetry

$$S(x, y, p_x, p_y) = (x, -y, -p_x, p_y).$$

For the flow $\phi(t, q)$ of (2.3) we have

$$S(\phi(t, q)) = \phi(-t, S(q)). \quad (2.5)$$

We will say that an orbit $q(t)$ is S -symmetric when

$$S(q(t)) = q(-t). \quad (2.6)$$

Each Lyapunov orbit is S -symmetric. It possesses a two dimensional stable manifold and a two dimensional unstable manifold. These manifolds lie on the same energy level as the orbit and their intersection, when restricted to the three dimensional constant energy manifold (2.4), is transversal. These invariant manifolds are S -symmetric with respect to each other, meaning that the stable manifold is an image by S of the unstable manifold (see Figure 2.3 for the unstable manifold, and Figure 2.4 for the intersection of manifolds). All these facts are well known and extensively studied numerically.

Our aim in this paper will be firstly to provide a rigorous-computer-assisted proof of existence of the manifold of Lyapunov orbits over a large radius from L_2 (see Figure 2.2). Secondly, using rigorous-computer-assisted computations, we shall show that for orbits with energies close to the energy of comet Oterma $h = 1.515$ their associated stable and unstable manifolds intersect transversally. Even though such intersections are well known from numerical investigation, to the best of our knowledge this is a first rigorous proof of their existence.

2.2. Interval Newton Method. Let X be a subset of \mathbb{R}^n . We shall denote by $[X]$ an interval enclosure of the set X , that is, a set

$$[X] = \prod_{i=1}^n [a_i, b_i] \subset \mathbb{R}^n,$$

such that

$$X \subset [X].$$

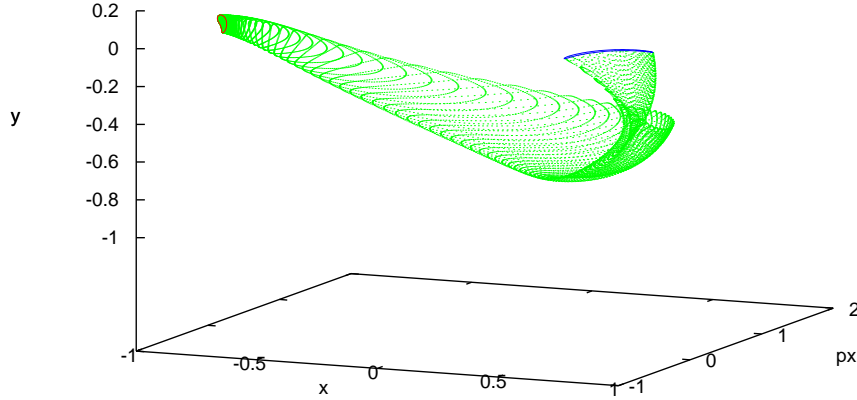


FIG. 2.3. The Lyapunov orbit in red, its unstable manifold in green, and the intersection of the unstable manifold with section $\{y = 0\}$ in blue, projected onto x, y, p_x coordinates. The figure is for the energy of comet Oterma $h = 1.515$ in the Jupiter-Sun system.

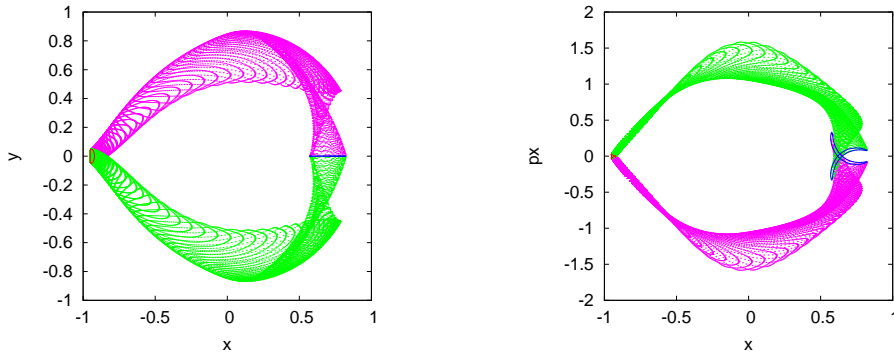


FIG. 2.4. The Lyapunov orbit in red, its unstable manifold in green, stable manifold in purple, and their intersections with section $\{y = 0\}$ in blue, projected onto x, y coordinates (left) and x, p_x coordinates (right). The figure is for the energy of comet Oterma $h = 1.515$ in the Jupiter-Sun system.

Let $f : \mathbb{R}^n \rightarrow \mathbb{R}^n$ be a C^1 function and $U \subset \mathbb{R}^n$. We shall denote by $[Df(U)]$ the interval enclosure of a Jacobian matrix on the set U . This means that $[Df(U)]$ is an interval matrix defined as

$$[Df(U)] = \left\{ A \in \mathbb{R}^{n \times n} \mid A_{ij} \in \left[\inf_{x \in U} \frac{df_i}{dx_j}(x), \sup_{x \in U} \frac{df_i}{dx_j}(x) \right] \text{ for all } i, j = 1, \dots, n \right\}.$$

THEOREM 2.1. [2] (*Interval Newton method*) Let $f : \mathbb{R}^n \rightarrow \mathbb{R}^n$ be a C^1 function and $X = \prod_{i=1}^n [a_i, b_i]$ with $a_i < b_i$. If $[Df(X)]$ is invertible and there exists an x_0 in X such that

$$N(x_0, X) := x_0 - [Df(X)]^{-1} f(x_0) \subset X,$$

then there exists a unique point $x^* \in X$ such that $f(x^*) = 0$.

2.3. Notations. Throughout the paper we shall use a notation $\phi(t, x)$ for the flow, and $\Phi_T(x) = \phi(T, x)$ for a time T shift along trajectory map of (2.3). For points $p = (x, y)$ we shall write $\pi_x p$ and $\pi_y p$, to denote projections onto coordinates x and y respectively. We shall also use the following notation for a cartesian product of sets $\prod_{i=1}^n U_i = U_1 \times \dots \times U_n$. For $A, B \subset \mathbb{R}^n$ we shall use a notation $A + B = \{a + b | a \in A, b \in B\}$.

3. Existence of a Family of Lyapunov Orbits. In this section we shall present a method for proving existence of Lyapunov orbits far away from L_2 . The result is in the spirit of the method applied by Wilczak and Zgliczyński in [19, 20] for a Lyapunov orbit with energy $h = 1.515$ of the comet Oterma. Our result differs from [19, 20] by the fact that we obtain a smooth family of orbits over a large set, whereas in [19, 20] a single orbit was proved.

We shall consider orbits starting from points of the form $(x, 0, 0, p_y)$ with x inside an interval

$$\begin{aligned} I_x &= [\underline{I}_x, \overline{I}_x] := \left[\frac{1}{2}(-1 + \mu - 0.933), -0.933 \right] \\ &\approx [-0.96602315, -0.933] \subset \mathbb{R}. \end{aligned} \quad (3.1)$$

Since $\pi_x L_2 \approx -0.93237$ we see that $\underline{I}_x < \frac{1}{2}(-1 + \mu - \pi_x L_2)$, so the interval I_x stretches from half the distance between the smaller primary and L_2 , almost up to L_2 (see Figure 2.2, where the orbits are depicted in green, and stretch between an inner and outer orbit depicted in blue).

Let us consider a section $\Sigma = \{y = 0\}$ and a Poincaré map $P : \Sigma \rightarrow \Sigma$ of (2.3). We shall interpret the Poincaré map as a function from \mathbb{R}^3 to \mathbb{R}^3 with coordinates x, p_x, p_y . If for a point $q = (x, 0, p_y) \in \Sigma$ we have $\pi_{p_x} P(q) = 0$, then by the symmetry property (2.5) the point q lies on a periodic orbit (the Poincaré map P makes a half turn along the orbit starting from q).

Let us introduce the following notation

$$f : \mathbb{R}^2 \rightarrow \mathbb{R},$$

$$f(x, p_y) = \pi_{p_x} P(x, 0, p_y).$$

To find a periodic orbit for some fixed x it is sufficient to find a zero of a function

$$g_x(p_y) := f(x, p_y).$$

Let $DP = (dP_{ij})_{i,j=1,2,3}$ be the derivative of the map P , with indexes 1, 2, 3 corresponding to coordinates x, p_x, p_y respectively.

LEMMA 3.1. Let I and J_i for $i = 0, 1$ be closed intervals such that J_0, J_1 have the same center point p_y^0 and $J_0 \subset J_1$. Let x^0 be the center point of I . Let $a \in \mathbb{R}$ and

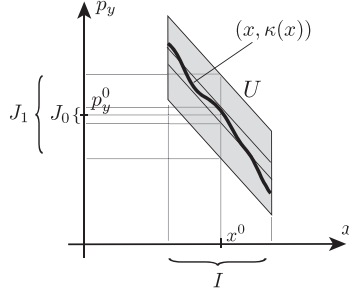


FIG. 3.1. The bound for a curve of points $q(x) = (x, 0, 0, \kappa(x))$ on Lyapunov orbits.

$U_0, U \subset \Sigma = \mathbb{R}^3$ be sets defined as (see Figure 3.1)

$$\begin{aligned} U_0 &= \{x^0\} \times \{0\} \times J_0, \\ U &= \{(x, 0, p_y) | x \in I, p_y = a(x - x^0) + \iota, \iota \in J_1\}. \end{aligned} \quad (3.2)$$

If

$$N := p_y^0 - \left[\frac{\pi_{p_x} P(x^0, 0, p_y^0)}{dP(U)_{23}} \right] \subset J_0, \quad (3.3)$$

and

$$|\alpha - a| < \frac{1}{|I|} (|J_1| - |J_0|) \quad \text{for all } \alpha \in [\underline{\alpha}, \bar{\alpha}] := \left[-\frac{dP(U)_{21}}{dP(U)_{23}} \right], \quad (3.4)$$

then there exists a smooth function $\kappa : I \rightarrow \mathbb{R}$ such that for any $x \in I$ a point $q(x) = (x, 0, 0, \kappa(x))$ lies on an S -symmetric periodic orbit of (2.3). Moreover, $\kappa'(x) \in [\underline{\alpha}, \bar{\alpha}]$ and $q(x) \in U$ for all $x \in I$.

Proof. Existence of a unique point $\kappa(x_0) \in J_0$ for which $g_{x_0}(\kappa(x_0)) = 0$ follows from (3.3), which implies

$$p_y^0 - [Dg_{x_0}(J_0)]^{-1} g_{x_0}(p_y^0) \subset N \subset J_0,$$

combined with interval Newton method (Theorem 2.1).

For (3.4) to hold we need to have $0 \notin dP(U)_{23}$. For $(x, 0, p_y) \in U$ we have $\frac{\partial f}{\partial p_y}(x, p_y) \in dP(U)_{23}$ hence $\frac{\partial f}{\partial p_y}(x, p_y) \neq 0$. This means that we can apply the implicit function theorem to obtain a curve $\kappa(x)$ for which $f(x, \kappa(x)) = 0$. We now need to make sure that the curve κ is defined on the entire interval I . At each point x for which $(x, 0, \kappa(x)) \in U$ is defined, by the implicit function theorem we know that

$$\kappa'(x) = -\frac{\frac{\partial f}{\partial x}(x, \kappa(x))}{\frac{\partial f}{\partial p_y}(x, \kappa(x))} \in \left[-\frac{dP(U)_{21}}{dP(U)_{23}} \right].$$

This, by assumption (3.4), means that we can continue the curve from $\kappa(x^0)$ to the whole interval I (see Figure 3.1). \square

To apply Lemma 3.1 we first compute numerically a sequence of points (see Figure 3.2)

$$\begin{aligned} q_i^0 &= (x_i^0, 0, 0, p_{y,i}^0) \quad \text{for } i = 0, \dots, 15000, \\ x_i^0 &= \underline{I_x} + \frac{i}{15000} (\overline{I_x} - \underline{I_x}), \end{aligned}$$

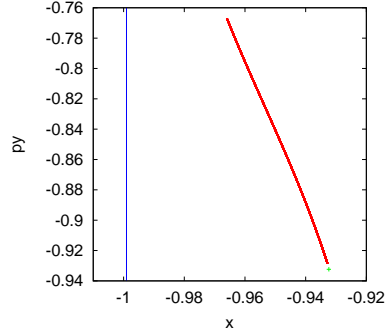


FIG. 3.2. Numerical plot of $\kappa(x)$, consisting of 15 000 points q_i^0 on Lyapunov orbits (in red). The point L_2 is in green. The blue line $x = -1 + \mu$ gives an indication of the position of the smaller primary along the x coordinate.

where $\underline{I}_x, \overline{I}_x$ are defined in (3.1). The q_i^0 are non-rigorously, numerically computed points on Lyapunov orbits. We then compute (non-rigorously) a sequence of slopes (see Figure 3.3)

$$a_i \in \mathbb{R} \quad i = 0, \dots, 15\,000,$$

define

$$r = \frac{1}{15\,000} \frac{1}{2} (\overline{I}_x - \underline{I}_x) \approx 10^{-6} \cdot 1.1007716,$$

$$\begin{aligned} I_i &= x_i^0 + [-r, r], \\ J_{0,i} &= p_{y,i}^0 + 10^{-13} \cdot [-1, 1], \\ J_{1,i} &= p_{y,i}^0 + 10^{-8} \cdot [-5, 5], \end{aligned}$$

and consider sets

$$\begin{aligned} U_0 &= \{x_i^0\} \times \{0\} \times J_{0,i}, \\ U_i &= \{(x, 0, p_y) \mid x \in I_i, p_y = a_i(x - x_i^0) + \iota, \iota \in J_{1,i}\}. \end{aligned}$$

We apply Lemma 3.1 repeatedly 15 000 times, and obtain the following theorem.

THEOREM 3.2 (First main result). *Let I_x be the interval from (3.1). Then there exists a curve $q(x) = (x, 0, 0, \kappa(x))$ of points on Lyapunov orbits with $\kappa : I_x \rightarrow \mathbb{R}$, which lies within a $5 \cdot 10^{-8}$ distance from the piecewise linear curve joining the 15 000 points q_i^0 on Figure 3.2.*

The proof of Theorem 3.2 took 5 hours and 43 minutes on a standard laptop.

REMARK 3.3. *Using above described method it is impossible to continue with the orbits to L_2 . At the fixed point one would need to apply alternative methods, such as the method of majorants [18], Lyapunov theorem by tracing the radius of convergence of the normal form [17], or topological-computer-assisted tools such as [5, 7].*

4. Outline of Results for Intersections of Invariant Manifolds. In the remainder of the paper we shall focus our attention on orbits starting from $q(x) = (x, 0, 0, \kappa(x))$ with $x \in I$ for

$$\begin{aligned} I &= [\underline{I}, \overline{I}] := x^0 + [-1, 1] \cdot 10^{-9}, \\ x^0 &= -0.9510055339445208. \end{aligned} \tag{4.1}$$

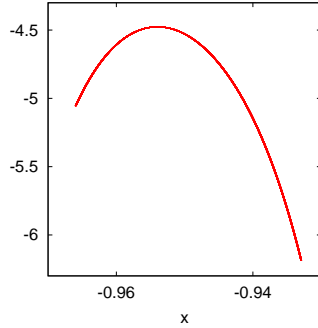


FIG. 3.3. Numerical plot of $\kappa'(x)$, consisting of 15 000 points a_i

Such orbits have energy close to the energy of the comet Oterma $h = 1.515$.

Let us introduce a notation Λ for a family of Lyapunov orbits, which start from $q(x)$ with $x \in I$

$$\Lambda = \{\phi(t, q(x)) | t \in \mathbb{R}, q(x) = (x, 0, 0, \kappa(x)), x \in I\}. \quad (4.2)$$

For $x \in I$, let $L(x) \subset \Lambda$ denote the Lyapunov orbit which starts from $q(x)$.

Throughout the remainder of the paper we shall prove the following theorem.

THEOREM 4.1 (Second main result). *Λ is a normally hyperbolic invariant manifold with a boundary. Each orbit $L(x) \subset \Lambda$ possesses a two dimensional stable manifold $W^s(L(x))$ and a two dimensional unstable manifold $W^u(L(x))$. The manifolds $W^s(L(x))$ and $W^u(L(x))$ intersect and the intersection, when restricted to the constant energy manifold $M(H(L(x)))$, is transversal (see (2.4) for definition of M).*

Numerical plots of the intersection of manifolds that we shall prove are given in Figure 2.4.

Theorem 4.1 will be proved with computer assistance. During the proof we shall obtain rigorous bounds on the region and the angle at which the manifolds intersect (see Figure 7.6).

The size of interval I (4.1) is very small. When translated the real life distance in the Jupiter-Sun system, its length is just slightly over one and a half kilometer. This is practically a single point. We need to start with such a small set to obtain our result. Thanks to this we obtain sharp estimates on the intersection of $W^s(L(x))$, $W^u(L(x))$. To consider a larger set of Lyapunov orbits one would need to iterate the procedure a number of times. This can be done without any difficulty apart from necessary time for computation. The proof of Theorem 4.1 took 46 minutes on a standard laptop. Using clusters one could cover a larger interval I in reasonable time.

5. Hyperbolicity of Lyapunov Orbits and Foliation by Energy. In this section we shall show that each orbit $L(x) \subset \Lambda$ lies on a different energy level. We shall also show that each orbit $L(x)$ (when considered on its constant energy manifold) is hyperbolic. In other words, we shall show that Λ is a normally hyperbolic manifold with a boundary.

We start with a simple remark.

REMARK 5.1. *If for all $x \in I$ we have $\frac{d}{dx}H(q(x)) \neq 0$, then Lyapunov orbits with different x have different energies. Note that the set U and the bound on the*

derivative of $\kappa'(x)$ from Lemma 3.1 can be used to obtain

$$\frac{d}{dx}H(q(x)) \in \left[\frac{\partial H}{\partial x}(U) + \frac{\partial H}{\partial p_y}(U)\kappa'(U) \right].$$

We shall now give a simple lemma which can be used to show that our Lyapunov orbits are hyperbolic.

In what follows in this section, let $P : \Sigma \rightarrow \Sigma$ be a second return Poincaré map for $\Sigma = \{y = 0\}$. This means that each point $q(x) = (x, 0, 0, \kappa(x))$, with $x \in I$, is a fixed point of P . We shall interpret the Poincaré map as a function from \mathbb{R}^3 to \mathbb{R}^3 with coordinates x, p_x, p_y .

LEMMA 5.2. *Let U be the set given by (3.2) in Lemma 3.1. Assume that for any 1×2 matrix A*

$$A \in \left[\left(- \left(\frac{\partial H}{\partial x} \right)^{-1} \begin{pmatrix} \frac{\partial H}{\partial p_x} & \frac{\partial H}{\partial p_y} \end{pmatrix} \right) (U) \right] \quad (5.1)$$

and any 2×2 matrix B

$$B \in \left[\left(\begin{pmatrix} dP_{21} & \\ dP_{31} & \end{pmatrix} A + \begin{pmatrix} dP_{22} & dP_{23} \\ dP_{32} & dP_{33} \end{pmatrix} \right) (U) \right] \quad (5.2)$$

the spectrum of B consists of two real eigenvalues λ_1, λ_2 satisfying $|\lambda_1| > 1 > |\lambda_2|$. Then for any $x \in I$ the Lyapunov orbit starting from $q(x)$, restricted to the constant energy manifold $M(H(q(x)))$, is a hyperbolic orbit.

Proof. Let us fix some $\hat{x} \in I$. For our assumptions to hold, A from (5.1) needs to be properly defined. This means that $\frac{\partial H}{\partial x}(q(\hat{x})) \neq 0$. By the implicit function theorem there exists a function $x(p_x, p_y)$ with $x(0, \kappa(\hat{x})) = \hat{x}$ such that $H(x(p_x, p_y), 0, p_x, p_y) = H(q(\hat{x}))$ and

$$\begin{pmatrix} \frac{\partial x}{\partial p_x} & \frac{\partial x}{\partial p_y} \end{pmatrix} (0, \kappa(\hat{x})) = - \left(\frac{1}{\frac{\partial H}{\partial x}} \begin{pmatrix} \frac{\partial H}{\partial p_x} & \frac{\partial H}{\partial p_y} \end{pmatrix} \right) (0, \kappa(\hat{x})). \quad (5.3)$$

The Lyapunov orbit starting from $q(\hat{x})$ is contained in the constant energy manifold $M(H(q(\hat{x})))$. Let us consider $V = M(H(q(\hat{x}))) \cap \{y = 0\}$ and a Poincaré map $\tilde{P} : V \rightarrow V$. In a neighborhood of $q(\hat{x})$ the manifold V can be parameterized by (p_x, p_y) . Since

$$\tilde{P}(p_x, p_y) = \pi_{(p_x, p_y)} P(x(p_x, p_y), p_x, p_y)$$

we have

$$\begin{aligned} D\tilde{P}(0, \kappa(\hat{x})) & \\ &= \left(\left(\pi_{(p_x, p_y)} \frac{\partial P}{\partial x} \right) \begin{pmatrix} \frac{\partial x}{\partial p_x} & \frac{\partial x}{\partial p_y} \end{pmatrix} + \begin{pmatrix} dP_{22} & dP_{23} \\ dP_{32} & dP_{33} \end{pmatrix} \right) (\hat{x}, 0, \kappa(\hat{x})). \end{aligned} \quad (5.4)$$

By (5.3), (5.4) and our assumption about the spectrum of B of from (5.2), follows that $(0, \kappa(\hat{x}))$ is a hyperbolic fixed point for the map \tilde{P} . This means that the Lyapunov orbit starting from $q(\hat{x})$, restricted to the constant energy manifold $M(H(q(\hat{x})))$ is hyperbolic. \square

REMARK 5.3. *Since B from (5.2) is a 2×2 matrix, estimation of its eigenvalues is straightforward. Here we profit from the the reduction of dimension made by restricting to a constant energy manifold.*

Since we consider a small part of the family of orbits (4.1), we can obtain a much tighter enclosure of the curve $\kappa(x)$ for $x \in I$ than from Theorem 3.2. Let

$$\begin{aligned} p_y^0 &= -0.836804179646973 & J_0 &= p_y^0 + [-1, 1] \cdot 10^{-13} \\ a &= -4.506866203376769 & J_1 &= p_y^0 + [-1, 1] \cdot 10^{-12} \end{aligned} \quad (5.5)$$

and

$$U = \{(x, 0, 0, p_y) \mid x \in I, p_y = a(x - x^0) + \iota, \iota \in J_1\}. \quad (5.6)$$

PROPOSITION 5.4. *For $x \in I$, with I from (4.1), we have $q(x) = (x, 0, 0, \kappa(x)) \subset U$ and*

$$\kappa'(x) \in [-4.506980818, -4.506751634], \quad (5.7)$$

$$\frac{d}{dx}H(q(x)) \in [-0.3670937615, -0.3670674516], \quad (5.8)$$

$$H(\underline{I}, 0, 0, a(\underline{I} - x_0) + J_1) \in [-1.514999999635, -1.514999999631],$$

$$H(\bar{I}, 0, 0, a(\bar{I} - x_0) + J_1) \in [-1.515000000369, -1.515000000365].$$

Moreover, the orbits (when considered on their constant energy manifolds) are hyperbolic, and we have following bounds for the eigenvalues

$$\lambda_1 \in [1450.24, 1481.68], \quad (5.9)$$

$$\lambda_2 \in 10^{-4} [6.74909, 6.89541].$$

Proof. The proof was performed with computer assistance. It required no subdivision of U and the computation took less than two seconds on a standard laptop.

Existence of $q(x) \subset U$ was shown using Lemma 3.1. From it also follows the bound (5.7) for $\kappa'(x)$. The bound (5.8) follows from Remark 5.1. Hyperbolicity and bounds (5.9) follow from Lemma 5.2. \square

6. Cone Conditions and Bounds for Unstable Manifolds of Saddle-Center Fixed Points. In this section we provide a topological tool that can be used for rigorous-computer-assisted detection of unstable manifolds of saddle-center fixed points. The method is a modification of [21], where instead of saddle-center a standard hyperbolic fixed point was considered. The content of this section is a general result. In section 7 we return to the PRC3BP and show how to apply it for the proof of Theorem 4.1.

Let $F : \mathbb{R}^n \rightarrow \mathbb{R}^n$ be a C^k diffeomorphism with a fixed point $v^* \in \mathbb{R}^n$ and $k \geq 1$. Assume that for eigenvalues $\lambda_1, \lambda_2, \dots, \lambda_n$ from the spectrum of $DF(v^*)$ we have

$$\begin{aligned} |\operatorname{re}\lambda_1| &> m > 1, \\ |\operatorname{re}\lambda_i| &< m \quad \text{for } i = 2, \dots, n. \end{aligned} \quad (6.1)$$

Let $W^u(v^*)$ denote the unstable manifold of v^* associated with the eigenvalue λ_1

$$W^u(v^*) = \{v \mid \|F^{-n}(v) - v^*\| < Cm^{-n} \text{ for all } n \in \mathbb{N} \text{ and some } C > 0\}.$$

Let $u = 1$ and $c = n - 1$. The notations u and c will stand for "unstable" and "central" coordinates of F at v^* . Consider two balls B_u and B_c , of dimensions u and

c respectively, such that $B_u \times B_c$ is centered at v^* . For a point $v \in \mathbb{R}^u \times \mathbb{R}^c$ we shall write $v = (x, y)$, with $x \in \mathbb{R}^u$, $y \in \mathbb{R}^c$. In these notations we shall also write the fixed point as $v^* = (x^*, y^*)$.

REMARK 6.1. *We do not need to assume that $(x, 0)$ is the eigenvector associated with λ_1 and that vectors $(0, y)$ span the eigenspace of $\lambda_2, \dots, \lambda_n$. For our method to work it is enough if these vectors are "roughly" aligned with the eigenspaces. This is important for us, since in any computer assisted computation it is usually not possible to compute the eigenvectors with full precision.*

Let $\alpha \in \mathbb{R}$, $\alpha > 0$ and consider a function $Q : \mathbb{R}^u \times \mathbb{R}^c \rightarrow \mathbb{R}$

$$Q(x, y) = \alpha x^2 - \|y\|^2.$$

For $v_0 \in \mathbb{R}^u \times \mathbb{R}^c$ we shall use a notation $Q^+(v_0)$ for a cone

$$Q^+(v_0) = \{v | Q(v - v_0) \geq 0\}.$$

Let us assume that α is chosen sufficiently small so that $Q^+(v^*) \cap B_u \times B_c$ does not intersect with $B_u \times \partial B_c$ (See Figure 6.1).

DEFINITION 6.2. *We shall say that $h : B_u \rightarrow B_u \times B_c$ is a horizontal disc in $B_u \times B_c$ for cones given by Q if $h(x^*) = v^*$, $\pi_x h(x) = x$ and for any $x_1 \neq x_2$ holds $Q(h(x_1) - h(x_2)) > 0$.*

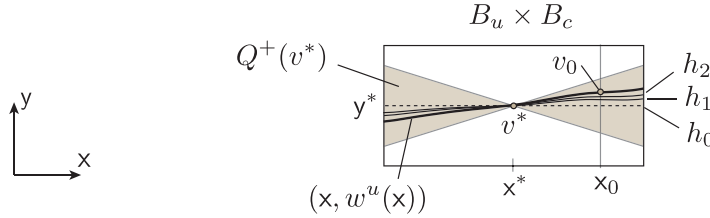


FIG. 6.1. Construction of the curve $(x, w^u(x))$ which lies on the unstable manifold of v^* .

LEMMA 6.3. *Assume that for any $v_1, v_2 \in Q^+(v^*)$, such that $Q(v_1 - v_2) \geq 0$, we have*

$$Q(F(v_1) - F(v_2)) > 0. \quad (6.2)$$

Let m be the constant from (6.1). If for any $v \in B$, $v \neq v^*$, $Q(v - v^*) \geq 0$ holds

$$\|F(v) - v^*\| > m \|v - v^*\|, \quad (6.3)$$

then $W^u(v^*) \subset Q^+(v^*)$. Moreover, there exists a function $w^u : B_u \rightarrow B_c$ such that $(id, w^u)(B_u) = W^u(v^*) \cap U$, and for any $x_1, x_2 \in B_u$, $x_1 \neq x_2$

$$Q((x_1, w^u(x_1)) - (x_2, w^u(x_2))) > 0 \quad (6.4)$$

and

$$\|(w^u)'(x)\| \leq \sqrt{\alpha} \quad \text{for all } x \in B_u. \quad (6.5)$$

Proof. We shall first show that for any $x_0 \in B_u \setminus \{x^*\}$ there exists a point $v_0 = (x_0, w^u(x_0)) \in Q^+(v^*)$ such that $v_0 \in W^u(v^*)$. Let $h_0(x) = (x, y^*)$ be a horizontal disc (See Figure 6.1). Observe that $F(h_0(x^*)) = F(x^*, y^*) = v^*$. By assumptions

(6.2), (6.3) the curve $F(h_0(x))$ is contained in $Q^+(v^*)$ and $F(h_0(\partial B_u)) \cap B_u \times B_c = \emptyset$. Moreover, by assumption (6.2) for any $x_1, x_2 \in B_u$, $x_1 \neq x_2$

$$Q(F(h_0(x_1)) - F(h_0(x_2))) > Q(h_0(x_1) - h_0(x_2)) > 0,$$

which means that $\{F(h_0(x)) | x \in B_u\} \cap B_u \times B_c$ is a graph of a horizontal disc. Let us denote this disc by h_1 and observe that $h_1(x^*) = v^*$. In other words, let h_1 be the graph transform of the disc h_0 .

Taking $F(h_1(x))$ and applying an identical argument, we observe that

$$\{F(h_1(x)) | x \in B_u\} \cap B_u \times B_c$$

is a graph of a horizontal disc h_2 . Repeating this procedure we can construct a sequence of horizontal discs h_0, h_1, h_2, \dots . For a fixed x_0 , due to compactness of closure of B_c , there exists a subsequence $h_{k_i}(x_0)$ convergent to some point $v_0 \in B_u \times \text{cl}B_c$. For any $i, n \in \mathbb{N}$ with $k_i > n$ the point $F^{-n}(h_{k_i}(x_0))$ lies on the graph of h_{k_i-n} and hence is also in $Q^+(v^*)$. This means that for any $n \in \mathbb{N}$

$$F^{-n}(v_0) = \lim_{i \rightarrow \infty} F^{-n}(h_{k_i}(x_0)) \in Q^+(v^*).$$

By assumption (6.3) we have

$$\|F^{-n}(v_0) - v^*\| < \frac{1}{m^n} \|v_0 - v^*\|,$$

which means that $v_0 \in W^u(v^*)$. By construction $\pi_x v_0 = x_0$, hence we can define $w^u(x_0) := \pi_y v_0$.

By the stable/unstable manifold theorem, there exists a small interval $I_\varepsilon = (x^* - \varepsilon, x^* + \varepsilon)$ in which $\{(x, w^u(x)) | x \in I_\varepsilon\}$ is a C^k curve which gives full description of $W^u(v^*)$. Since $(x, w^u(x)) \subset Q^+(v^*)$ we have $(1, (w^u)'(x^*)) \in Q^+(0)$. Since for sufficiently small ε the vector $(1, (w^u)'(x))$ is arbitrarily close to $(1, (w^u)'(x^*))$, for $x_1, x_2 \in I_\varepsilon$

$$Q((x_1, w^u(x_1)) - (x_2, w^u(x_2))) > 0. \quad (6.6)$$

Iterating the curve $(x, w^u(x))$ through F , by (6.2), (6.3) we obtain our function $w^u : B_u \rightarrow B_c$. Note that by our construction for any $x_1, x_2 \in B_u$ inequality (6.6) holds. This implies that for any $x_1, x_2 \in B_u$

$$\frac{\|w^u(x_1) - w^u(x_2)\|^2}{|x_1 - x_2|^2} < \alpha,$$

which in turn gives (6.5). \square

REMARK 6.4. Lemma 6.3 can easily be generalized to higher dimension of $W^u(v^*)$. The proof would be identical, taking $Q(x, y) = \alpha\|x\|^2 - \|y\|^2$. Here we have set up our discussion so that $W^u(v^*)$ is one dimensional simply because this is what we shall need for our application to the PRC3BP.

REMARK 6.5. By taking the inverse map, Lemma 6.3 can be used to prove existence of stable manifolds.

To verify assumptions (6.2) and (6.3) in practice, it is best to make use of an interval matrix $\mathbf{A} = [DF(Q^+(v^*))]$. Then for any $v_1, v_2 \in Q^+(v^*)$ we have

$$F(v_1) - F(v_2) = \int_0^1 DF(v_2 + t(v_1 - v_2)) dt \cdot (v_1 - v_2) \in \mathbf{A}(v_1 - v_2). \quad (6.7)$$

This means that

$$F(v) - v^* \subset \mathbf{A}(v - v^*). \quad (6.8)$$

To verify (6.3) using (6.8) we can apply Lemma 10.1 from the Appendix.

Let us now turn to verification of (6.2). Let C_Q be a diagonal matrix such that $v^T C_Q v = Q(v)$. Equation (6.7) gives an estimate

$$Q(F(v_1) - F(v_2)) \subset (v_1 - v_2)^T \mathbf{A}^T C_Q \mathbf{A} (v_1 - v_2). \quad (6.9)$$

To verify (6.2) using (6.9) we can apply Lemma 10.2 from the Appendix.

7. Rigorous Bounds for Invariant Manifolds associated with Lyapunov Orbits. In this section we give a proof of Theorem 4.1. In sections 7.1 and 7.2 we shall show how to apply the method from section 6 to detect fibers of unstable manifolds of Lyapunov orbits. In section 7.3 we shall show how to prove that the manifolds intersect. Using these results, in section 7.4 we give a computer assisted proof Theorem 4.1.

7.1. Parameterization Method. The method from section 6 requires a good change of coordinates which "straightens out" the unstable manifold. We shall obtain such a change of coordinates using a parameterization method. In this subsection we give an outline of this procedure.

In this section we shall fix some $x \in I$ and show how to find an unstable fiber of a point

$$q_0 = q(x) = (x, 0, 0, \kappa(x)) \in L(x).$$

We shall use a notation $\tau = \tau(q_0)$ for the return time along the trajectory. The point q_0 is a saddle center fixed point for a τ -time map $\Phi_\tau : \mathbb{R}^4 \rightarrow \mathbb{R}^4$.

Let C denote a matrix which brings $D\Phi_\tau(q_0)$ to real Jordan form. By $\tilde{\Phi}_\tau : \mathbb{R}^4 \rightarrow \mathbb{R}^4$ we shall denote the time τ map in the linearized local coordinates

$$\tilde{\Phi}_\tau(v) := C^{-1}(\Phi_\tau(q_0 + Cv) - q_0).$$

Let $W^u(\tilde{\Phi}_\tau, 0)$ denote the unstable manifold of $\tilde{\Phi}_\tau$ at zero. If we can find a function

$$K = (K_0, K_1, K_2, K_3) : \mathbb{R} \rightarrow \mathbb{R}^4,$$

which for all x in an interval $I_0 = [\underline{x}, \bar{x}]$, $\underline{x} < 0 < \bar{x}$, is a solution of a cohomology equation

$$\tilde{\Phi}_\tau(K(x)) = K(\lambda x), \quad (7.1)$$

then $K(x) \subset W^u(\tilde{\Phi}_\tau, 0)$ for $x \in I_0$.

Once K is established we can consider a nonlinear change of coordinates

$$\psi = (\psi_0, \psi_1, \psi_2, \psi_3) : \mathbb{R}^4 \rightarrow \mathbb{R}^4$$

defined as

$$\begin{aligned} \psi_0(x, y_1, y_2, y_3) &= K_0(x) - (y_1 K_1'(x) + y_2 K_2'(x) + y_3 K_3'(x)), \\ \psi_i(x, y_1, y_2, y_3) &= K_i(x) + y_i K_0'(x) \quad \text{for } i = 1, 2, 3. \end{aligned} \quad (7.2)$$

Note that $\psi(x, 0) = K(x)$ gives points on the unstable manifold of the fixed point for the map $\tilde{\Phi}_\tau$. The intuitive idea behind (7.2) is to orthogonalize coordinates around $K(x)$ (see Figure 7.1).

Let us define a local map

$$F = \psi^{-1} \circ \tilde{\Phi}_\tau \circ \psi.$$

Such map will play the role of F from section 6. Observe that

$$\{C\psi(K(x)) + q_0 | x \in I_0\} \subset C\psi(W^u(F, 0)) + q_0 = W^u(\tilde{\Phi}_\tau, q_0) \subset W^u(L(x_0)).$$

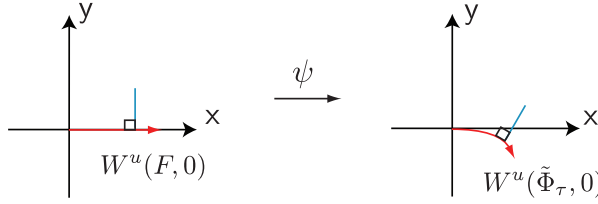


FIG. 7.1. The nonlinear change of coordinates ψ .

7.2. Bounds for Unstable Fibers through Parameterization and Cone conditions. The map ψ (7.2) gives us a change of coordinates which locally "straightens out" the unstable manifold. The problem with applying the procedure from section 7.1 in practice lies in the fact that usually finding an analytic formula for K satisfying (7.1) is impossible. The best that can be done is to find a K which is a polynomial approximation of a solution of (7.1). This can be done by expanding $\tilde{\Phi}_\tau$ into a Taylor series and inductively comparing the coefficients in (7.1) (for a detailed description of this method we refer the reader to [4]; see in particular Section 4 and Theorem 4.1). If we find such an approximate solution of (7.1), then the set $\{(x, 0) | x \in I_0\}$ is no longer the unstable manifold for F (defined by (7.3)), but its approximation. Even though then our description of the unstable fiber is not entirely accurate, we can apply the method from Section 6 to obtain a rigorous enclosure of $W^u(F, 0)$. This enclosure can then be transported to the original coordinates.

In this Section we shall assume that q_0 is an arbitrary point close to $q(x) = (x, 0, 0, \kappa(x))$ for $x \in I$, C is some given matrix and $K : \mathbb{R} \rightarrow \mathbb{R}^4$ is some given polynomial and that ψ is defined by (7.2).

REMARK 7.1. *Let us stress that the point q_0 is a numerical approximation of $q(x)$, the matrix C will be a (non-rigorous) numerically obtained estimate for the change into Jordan form of the map Φ_τ . We do not assume that this change is rigorously computed. This is practically impossible due to the fact that we do not have an analytic formula for $D\Phi_\tau(q_0)$. For us the matrix C is simply some approximation of the matrix which takes $D\Phi_\tau(q_0)$ into Jordan form. Let us note that it is not difficult to find an interval matrix \mathbf{C}^{-1} such that the inverse matrix of our C is contained in \mathbf{C}^{-1} .*

REMARK 7.2. *In our setting the polynomial K is an approximation of the solution of (7.1). In practice we cannot obtain a fully rigorous solution of (7.1). It is important to emphasize that we also do not have an inverse of ψ . It is also not simple to find good rigorous estimates for the function ψ^{-1} due to the fact that K is a high order polynomial. We shall therefore set up all our subsequent computations so that we will never need to use the inverse function of ψ .*

For $x \in I$, let $\tau(x)$ be the period of an orbit $L(x) \subset \Lambda$. We define a map

$$F = \psi^{-1} \circ \tilde{\Phi}_{\tau(x)} \circ \psi. \quad (7.3)$$

Note that for each $x \in I$ we have a different map F . We omit this in our notation for simplicity, and also because below methods for obtaining rigorous bounds for F and its derivative shall work for all $x \in I$.

We shall first be interested in computing rigorous bounds for $F(U)$. It turns out that (7.3) is impossible to apply since we do not have a formula for ψ^{-1} . Even if we did, direct application of (7.3) in interval arithmetic would provide very bad estimates due to strong hyperbolicity of the map. We use a more subtle method.

We shall first need the following notations. Let \mathbf{T} denote an interval such that $\tau(x) \in \mathbf{T}$ for all $x \in I$. Let $\lambda \in \mathbb{R}$ be some number close to an unstable eigenvalue of $D\Phi_{\tau(x)}(q(x))$ for some $x \in I$. We shall slightly abuse notations and also consider $\lambda : \mathbb{R}^4 \rightarrow \mathbb{R}^4$ as a function defined on $v = (x, y) \in \mathbb{R} \times \mathbb{R}^3$ as

$$\lambda(x, y) := (\lambda x, y).$$

The following Lemma allows us to obtain rigorous bounds on pre-images of F from (7.3).

LEMMA 7.3. *Let $U_1 \subset \mathbb{R}^4$ be a given set. Let $G : \mathbb{R} \times \mathbb{R}^4 \times \mathbb{R}^4 \rightarrow \mathbb{R}^4$ be defined as*

$$G(\tau, v_1, v_2) = \tilde{\Phi}_\tau(C\psi(v_1) + q_0) - (C\psi(\lambda(v_2)) + q_0). \quad (7.4)$$

Let $U_2 \subset \mathbb{R}^4$ be a set and $\mathbf{A}(U_2)$ be an interval matrix defined as

$$\mathbf{A}(U_2) = -[CD\psi(\lambda(U_2))D\lambda].$$

If

$$N(\mathbf{T}, v_0, U_1, U_2) := v_0 - [\mathbf{A}(U_2)]^{-1} [G(\mathbf{T}, U_1, v_0)] \subset U_2, \quad (7.5)$$

then

$$F(U_1) \subset \lambda(U_2). \quad (7.6)$$

Proof. The proof is given in the Appendix in section 10.2. See also Remark 10.4 for comments on practical application of the lemma. \square

REMARK 7.4. *The choice of the function G is motivated by the following diagram.*

$$\begin{array}{ccc} \mathbb{R}^4 & \xrightarrow{\Phi_\tau} & \mathbb{R}^4 \\ \uparrow C + q_0 & & \uparrow C + q_0 \\ \mathbb{R}^4 & \xrightarrow{\tilde{\Phi}_\tau} & \mathbb{R}^4 \\ \uparrow \psi & & \uparrow \psi \\ \mathbb{R}^4 & \left(\begin{array}{c} \lambda \\ \rightarrow \end{array} \right) & \mathbb{R}^4 \end{array}$$

The diagram is not fully commutative, hence the bracket for λ . Intuitively, for $v = (x, 0) \in \mathbb{R} \times \mathbb{R}^3$ the diagram should "almost commute". Even though this statement is nowhere close to rigorous, it might make the method and proof of Lemma 7.3 more intuitive.

We now turn to the computation of rigorous bounds for the derivatives of (7.3). For any (x, y) contained in a set $B \subset \mathbb{R}^4$ we have the following estimates

$$\begin{aligned} DF(x, y) &= (D\psi(F(x, y)))^{-1} C^{-1} D\Phi_{\tau(x)}(C\psi(x, y) + q_0) CD\psi(x, y) \\ &\subset \left[(D\psi(F(B)))^{-1} \right] \cdot [C^{-1}] \cdot [D\Phi_{\mathbf{T}}(C\psi(B) + q_0)] \cdot C \cdot [D\psi(B)] \\ &=: [DF(B)]. \end{aligned} \quad (7.7)$$

Note that to compute $[DF(B)]$ from (7.7) we do not need to use ψ^{-1} .

REMARK 7.5. *Using Lemma 7.3 and (7.7) we can in practice compute rigorous bounds for $[F(B)]$ and $[DF(B)]$. We perform such computations in Section 7.4.1 with the use of CAPD library (<http://capd.ii.uj.edu.pl/>). The library allows for computation of rigorous estimates for $\Phi_{\mathbf{T}}$ and its derivative and for rigorous-enclosure operations on maps and interval matrixes.*

Proposition 5.6 gives a bound on a set U (5.6) which contains all fixed points $q(x)$, with $x \in I$, of the map $\Phi_{\tau(x)}$. This set can be transported to local coordinates (x, y) . Let $B_0 \subset \mathbb{R}^4$ be such set that

$$\{\psi^{-1}(C^{-1}(q(x) - q_0)) \mid x \in I\} \subset B_0.$$

Such set can easily be computed using for example a technical Lemma 10.5 from the Appendix.

Taking a four dimensional set (see Figure 7.2)

$$B = \bigcup_{v \in B_0} Q^+(v) \subset \mathbb{R}^4$$

using (7.7) and Lemmas 10.1, 10.2 to verify assumptions of Lemma 6.3, we can obtain a bound for the unstable fibers of all $q(x)$ for $x \in I$. The obtained bound is computed in local coordinates (x, y) , but can easily be transported back to the original coordinates (x, y, p_x, p_y) of the system. Detailed results of such computation will be presented in section 7.4.1.

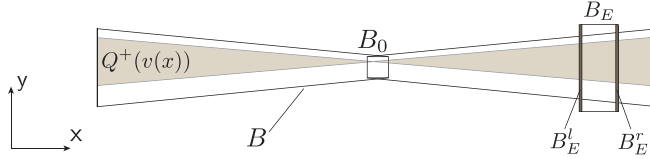


FIG. 7.2. *Local bound on the unstable manifold. Each fixed point $\psi^{-1}(C^{-1}(q(x) - q_0))$, for $x \in I$, lies in B_0 and its unstable manifold is contained in $B = \bigcup_{v \in B_0} Q^+(v)$.*

REMARK 7.6. *Let us emphasize that to apply the method it is enough to use a single point q_0 , single matrix C and single nonlinear change ψ . It is not necessary to use different changes to local coordinates for different $x \in I$.*

REMARK 7.7. *Let us note that from the fact that $W^s(L(x))$ is S -symmetric to $W^u(L(x))$, without any effort we also obtain mirror bounds for fibers of $W^s(L(x))$.*

7.3. Transversal Intersections of Manifolds. In this section we discuss how the bounds for fibers of $q(x)$ discussed in section 7.2 can be used to prove transversal intersections of manifolds $W^u(L(x))$ and $W^s(L(x))$ for $L(x) \subset \Lambda$ (see (4.2) for definition of Λ).

Let $x^l, x^r \in \mathbb{R}$ be such that $x^l < x^r$ and $\pi_x B_0 < x^l, x^r$. Let $B_c \subset \mathbb{R}^3$ be such that $\pi_y B \subset B_c$. Let B_E, B_E^l, B_E^r be defined as (see Figure 7.2)

$$\begin{aligned} B_E &= [x^l, x^r] \times B_c, \\ B_E^l &= \{x^l\} \times B_c, \\ B_E^r &= \{x^r\} \times B_c, \end{aligned}$$

and let

$$\begin{aligned} V^+ &= \{(x, y_1, y_2, y_3) \in \mathbb{R}^4 \mid x = 1, y_i \in [-\sqrt{\alpha}, \sqrt{\alpha}] \text{ for } i = 1, 2, 3\}, \\ V^- &= \{(x, y_1, y_2, y_3) \in \mathbb{R}^4 \mid x = -1, y_i \in [-\sqrt{\alpha}, \sqrt{\alpha}] \text{ for } i = 1, 2, 3\}, \\ V &= \{\gamma v \mid v \in V^+, \gamma \geq 0\} \cup \{\gamma v \mid v \in V^-, \gamma \geq 0\}. \end{aligned}$$

Note that

$$Q^+(0) \subset V.$$

Consider a section

$$\Sigma = \{y = 0\} \cap \{x > 0\} \cap \{p_x^2 < 2(H(L(x)) + \Omega(x, y))\}.$$

This shall be a section where we detect the intersection of $W^u(L(x))$ and $W^s(L(x))$ (see Figures 2.3, 2.4). Let ϕ be the flow of (2.3) and define

$$\begin{aligned} \tau(q) &= \inf\{t > 0 : \phi(t, q) \in \Sigma\}, \\ \mathcal{G} : B_E &\rightarrow \Sigma, \\ \mathcal{G}(x, y) &= \phi(\tau(C\psi(x, y) + q^0), C\psi(x, y) + q^0). \end{aligned}$$

LEMMA 7.8. *Assume that for F defined in (7.3) assumptions of Lemma 6.3 hold. If also*

$$\pi_{p_x} \mathcal{G}(B_E^l) < 0, \quad \pi_{p_x} \mathcal{G}(B_E^r) > 0, \quad (7.8)$$

then for any $x \in I$ (with I defined in (4.1)) the manifolds $W^u(L(x))$ and $W^s(L(x))$ intersect.

Moreover, if for any $v^+ \in V^+$ and $v^- \in V^-$

$$\begin{aligned} \pi_x [D\mathcal{G}(B_E)] v^+ &> 0, & \pi_{p_x} [D\mathcal{G}(B_E)] v^+ &> 0, \\ \pi_x [D\mathcal{G}(B_E)] v^- &< 0, & \pi_{p_x} [D\mathcal{G}(B_E)] v^- &< 0, \end{aligned} \quad (7.9)$$

then for each fixed $x \in I$ the intersection is transversal on the constant energy manifold $M(H(L(x)))$ (see (2.4) for definition of M).

Proof. Let us fix an $x \in I$. First let us observe that because energy (2.2) is preserved, the manifold $M(L(x)) \cap \Sigma$ can be parameterized by x, p_x since

$$p_y = p_y(x, p_x) = \sqrt{2(H(L(x)) + \Omega(x, y)) - p_x^2} + x \quad (7.10)$$

is well defined.

By Lemma 6.3 we know that in local coordinates x, y the unstable fiber of $q(x)$ is a horizontal disc in B . This disc is a graph of a function $w^u : B_u \rightarrow B_c$ and for any $x_1, x_2 \in B_u$ such that $x_1 \neq x_2$

$$(x_1, w^u(x_1)) - (x_2, w^u(x_2)) \in Q^+(0) \subset V.$$

The disc also passes through the set B_E (see Figure 7.2).

In the statement of our lemma we implicitly assume that $\mathcal{G}(x, y)$ is well defined for $(x, y) \in B_E$. This means that

$$W^u(L(x)) \cap \Sigma \cap \mathcal{G}(B_E) = \{\mathcal{G}(x, w^u(x)) \mid x \in [x^l, x^r]\}. \quad (7.11)$$

Let us introduce a notation

$$\begin{aligned} w_\Sigma^u &: [x^l, x^r] \rightarrow \mathbb{R}^2, \\ w_\Sigma^u(x) &= \pi_{x, p_x} \mathcal{G}(x, w^u(x)). \end{aligned}$$

By (7.10) and (7.11) the curve $w_\Sigma^u(x)$ parametrizes a fragment of the intersection of $W^u(L(x))$ with Σ . By assumption (7.8)

$$\begin{aligned} \pi_{p_x} w_\Sigma^u(x^l) &= \pi_{p_x} \mathcal{G}(x^l, w^u(x^l)) \in \pi_{p_x} \mathcal{G}(\{x^l\} \times B_c) = \pi_{p_x} \mathcal{G}(B_E^l) < 0, \\ \pi_{p_x} w_\Sigma^u(x^r) &= \pi_{p_x} \mathcal{G}(x^r, w^u(x^r)) \in \pi_{p_x} \mathcal{G}(\{x^r\} \times B_c) = \pi_{p_x} \mathcal{G}(B_E^r) > 0, \end{aligned}$$

hence we have an $x^* \in (x^l, x^r)$ such that

$$\pi_{p_x} w_\Sigma^u(x^*) = 0.$$

The unstable manifold $W^s(L(x))$ is S -symmetric to $W^u(L(x))$. This means that a fragment of intersection of $W^s(L(x))$ with Σ is parameterized by

$$\begin{aligned} w_\Sigma^s &: [x^l, x^r] \rightarrow \mathbb{R}^2, \\ w_\Sigma^s(x) &= (\pi_x w_\Sigma^u(x), -\pi_{p_x} w_\Sigma^u(x)). \end{aligned} \quad (7.12)$$

Since $w_\Sigma^u(x^*) = w_\Sigma^s(x^*)$ manifolds $W^u(L(x))$ and $W^s(L(x))$ intersect at

$$q^* = \mathcal{G}(x^*, w^u(x^*)).$$

Now we turn to proving transversality of the intersection at q^* . By (7.10), around q^* the manifold $M(H(L(x)))$ is parameterized by x, y, p_x . Therefore in the proof of transversality we restrict to these coordinates. Since \mathcal{G} is well defined, $W^u(L(x))$ must transversally cross $\{y = 0\}$. By symmetry so does $W^s(L(x))$. We therefore only need to prove that $w_\Sigma^u(x)$ and $w_\Sigma^s(x)$ intersect transversally in \mathbb{R}^2 .

Let $x^+ \in (x^*, x^r]$, $\gamma = 1/(x^+ - x^*)$ and

$$v = \gamma ((x^+, w^u(x^+)) - (x^*, w^u(x^*))) \in V^+.$$

By the mean value theorem

$$w_\Sigma^u(x^+) - w_\Sigma^u(x^*) \in \pi_{x, p_x} \frac{1}{\gamma} [D\mathcal{G}(B_E)] v.$$

By (7.9) this implies that

$$\pi_x(w_\Sigma^u(x^+) - w_\Sigma^u(x^*)) > 0, \quad \pi_{p_x}(w_\Sigma^u(x^+) - w_\Sigma^u(x^*)) > 0. \quad (7.13)$$

By mirror arguments, for $x^- \in [x^l, x^*)$

$$\pi_x(w_\Sigma^u(x^-) - w_\Sigma^u(x^*)) < 0, \quad \pi_{p_x}(w_\Sigma^u(x^-) - w_\Sigma^u(x^*)) < 0. \quad (7.14)$$

From (7.13), (7.14) and (7.12) we see that $w_\Sigma^u(x)$ and $w_\Sigma^s(x)$ intersect transversally at $w_\Sigma^u(x^*) = w_\Sigma^s(x^*)$, which concludes our proof. \square

REMARK 7.9. *From proof of Lemma 7.8 follows that we have the following estimate on the slope of the curves $w_\Sigma^u(x)$*

$$\mathbf{a} = \left[\frac{\pi_{p_x} DG(B_E)V^+}{\pi_x DG(B_E)V^+} \right] \cup \left[\frac{\pi_{p_x} DG(B_E)V^-}{\pi_x DG(B_E)V^-} \right].$$

By S -symmetry of $W^u(L(x))$ and $W^s(L(x))$ the slope of $w_\Sigma^s(x)$ is in $-\mathbf{a}$.

Once we verify (7.8) then by checking that $\mathbf{a} > 0$ we know that assumption (7.9) needs to hold.

7.4. Proof of Theorem 4.1. In this section we write the computer assisted rigorous bounds, which we obtain using the method from sections 7.2, 7.3. As a result we obtain rigorous bounds for the position of fibers of $W^u(L(x))$ and for transversal intersection of $W^u(L(x))$ with $W^s(L(x))$. By this we obtain the proof of Theorem 4.1.

7.4.1. Bounds for Unstable Fibers. We start by writing out our changes of coordinates needed for application of Lemma 7.3 to the map (7.3) from section 7.2.

We first choose the point $q_0 = (x^0, 0, 0, p_y^0)$ with x^0, p_y^0 given in (4.1) and (5.5) respectively, i.e.

$$\begin{aligned} x^0 &= -0.9510055339445208, \\ p_y^0 &= -0.8368041796469730. \end{aligned}$$

We choose a matrix C as

$$C = \begin{pmatrix} 0.197841 & -0.197841 & 0 & 0.221884 \\ -0.221884 & -0.221884 & 0.773671 & 0 \\ 1 & 1 & -1 & 0 \\ -0.255717 & 0.255717 & 0 & -1 \end{pmatrix}$$

We then choose four polynomials

$$\begin{aligned} K_0(x) &= 0.1x - 0.0621591x^2 + 0.0375888x^3 - 0.0200645x^4 \\ K_1(x) &= 0.000533561x^2 - 0.00723085x^3 + 0.00827176x^4 \\ K_2(x) &= -0.0151949x^2 + 0.009304476x^3 - 0.00427633x^4 \\ K_3(x) &= 0.0269670x^2 - 0.0275820x^3 + 0.0203022x^4 \end{aligned}$$

which define the nonlinear change of coordinates ψ (see (7.2)). All of the above choices are dictated by (non-rigorous) numerical investigation. Above choice ensures that $C\psi(x, 0) + q_0$ gives a decent approximation of the position of the unstable fibers of $q(x)$ for $x \in I$ for I given in (4.1).

Now our computations start. We first compute the interval enclosure \mathbf{T} such that $\tau(q(x)) \in \mathbf{T}$ for all $x \in I$. The obtained result is

$$\mathbf{T} = [3.058882598, 3.058883224].$$

Next we compute a set B_0 such that (see Figure 7.2)

$$\psi^{-1}(C^{-1}(q(x) - q^0)) \subset B_0.$$

Such set can be obtained using a technical Lemma 10.5 included in the Appendix. We thus obtain

$$B_0 = \begin{pmatrix} [-7.91575e-12, 7.91575e-12] \\ [-7.91575e-12, 7.91575e-12] \\ [-9.29424e-19, 9.29424e-19] \\ [-4.50827e-08, 4.50827e-08] \end{pmatrix}.$$

REMARK 7.10. *Note that the set is flat along the third and stretched along the last coordinate. This is because we set up C and ψ so that the third coordinate is associated with the section $\{y = 0\}$ (on which lie $q(x)$) and that the last coordinate is associated with the direction of the curve $q(x) = (x, 0, 0, \kappa(x))$.*

We now choose the size of our investigated set B in local coordinates and choose the parameters for our cones (see Figure 7.2). We take

$$\alpha = 2.56 \cdot 10^{-6},$$

and consider only one branch of the unstable manifold considering

$$B = \bigcup_{v \in B_0} Q^+(v) \cap \{x \in [\underline{x}, \bar{x}]\} \quad (7.15)$$

with

$$\underline{x} = -1 \cdot 10^{-11}, \quad \bar{x} = 4.5 \cdot 10^{-6}.$$

The choice of \bar{x} is dictated by the size of the fiber we later need to consider to prove intersections of stable/unstable manifolds.

To compute a rigorous enclosure of $[DF(B)]$ using (7.7), we subdivide B into $N = 1200$ parts B_i along the x coordinate

$$B = \bigcup_{i=1}^N B_i.$$

Using Lemma 7.3 to obtain enclosures of $F(B_i)$, combined with (7.7) we compute estimates for $[DF(B_i)]$. Combining the estimates $[DF(B_i)]$ we obtain the following global estimate for $[DF(B)]$ (the result is displayed with very rough accuracy, ensuring true enclosure in rounding)

$$[DF(B)] = \begin{pmatrix} [1465.6, 1466.5] & [-0.353, 0.369] & [-0.285, 0.283] & [-0.300, 0.333] \\ [-0.361, 0.360] & [-0.360, 0.361] & [-0.290, 0.277] & [-0.319, 0.304] \\ [-0.138, 0.140] & [-0.139, 0.139] & [0.896, 1.120] & [0.458, 0.700] \\ [-0.201, 0.202] & [-0.202, 0.202] & [-0.171, 0.149] & [0.823, 1.172] \end{pmatrix}.$$

Finally, using $[DF(B)]$ and Lemmas 10.1, 10.2 we verify assumptions of Lemma 6.3. We thus obtain rigorous bounds for the position of the fibers. The computation of the enclosure of the fibers took 18 minutes on a standard laptop.

We plot the obtained bounds on fibers transported to the original coordinates of the system x, y, p_x, p_y in Figures 7.3, 7.4, 7.5. On the plots we present rigorous enclosures of three fibers starting from $q(x)$ with x on the edges and the middle of

interval I (with I chosen in (4.1)). This gives us an overview of the size of our fiber enclosures (left hand side of Figures 7.3, 7.4, 7.5). We can see that close to the set which contains $\{q(x) = (x, 0, 0, \kappa(x)) | x \in I\}$, which is depicted in green, the estimates on the fibers is sharp (right hand plots in Figures 7.3, 7.4, 7.5). We can see that our three considered fiber enclosures are very close to each other, but are still separated, which is visible after closeup on the left hand side plot in Figure 7.5.

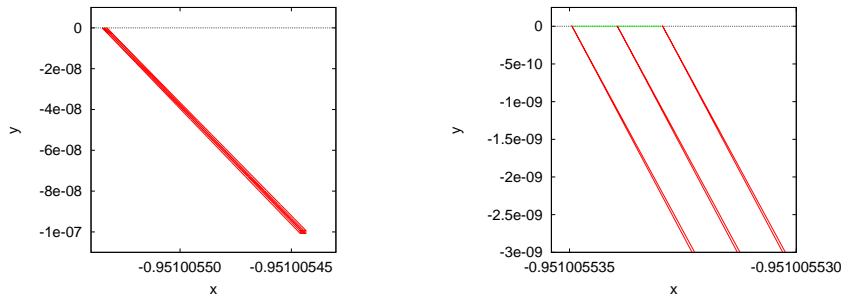


FIG. 7.3. Projections of fiber enclosures onto x, y coordinates.

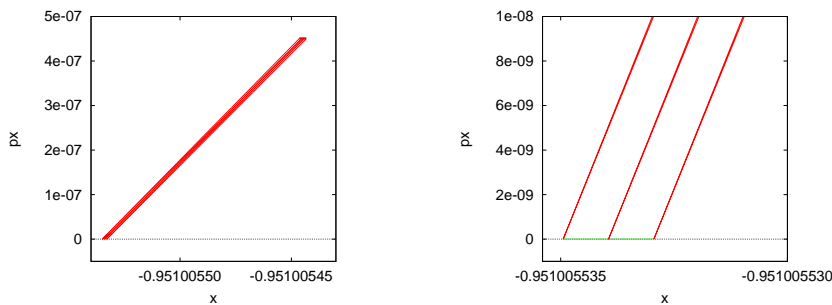


FIG. 7.4. Projections of fiber enclosures onto x, p_x coordinates.

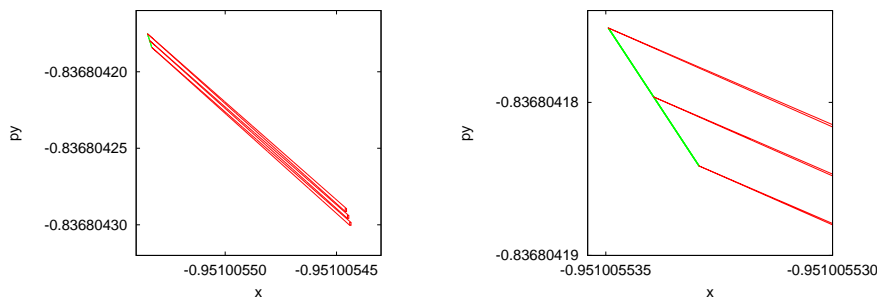


FIG. 7.5. Projections of fiber enclosures onto x, p_y coordinates.

REMARK 7.11. *The range of obtained fibers is small. It is possible to reach somewhat further from $q(x)$, but this significantly increases the time of computation, since further subdivision of the set is required.*

REMARK 7.12. *By using linearization only we have not been able to obtain ac-*

curate enough enclosure of the fibers to handle the proof of transversal intersection of manifolds which follows in section 7.4.2. Thus the use of higher order change of variables seems to be needed.

7.4.2. Bounds for Intersections of Manifolds. In this section we present rigorous-computer-assisted results in which we verify assumptions of Lemma 7.8 and thus conclude the proof of Theorem 4.1. For each $x \in I$ there are four points of intersection of $W^u(L(x))$ and $W^s(L(x))$ on $\{y = 0\}$. They can be seen on the left hand plot in Figure 7.6. We consider only the point which is furthestmost to the right.

We define the set $B_E = [x^l, x^r] \times B_c$ with x^l, x^r chosen as

$$x^m = 4.461867506615821 \cdot 10^{-6},$$

$$x^l = x^m - 10^{-11}, \quad x^r = x^m + 10^{-11}.$$

We verify that assumption (7.8) of Lemma 7.8 holds by computing $\mathcal{G}(B_E^l)$ and $\mathcal{G}(B_E^r)$. We plot the obtained bounds in red on the right hand side plot of Figure 7.6.

Next, using Remark 7.9 we compute

$$\mathbf{a} = [1.7695, 1.7725], \quad (7.16)$$

hence assumption (7.9) of Lemma 7.8 holds. Applying Lemma 7.8 concludes the proof of Theorem 4.1.

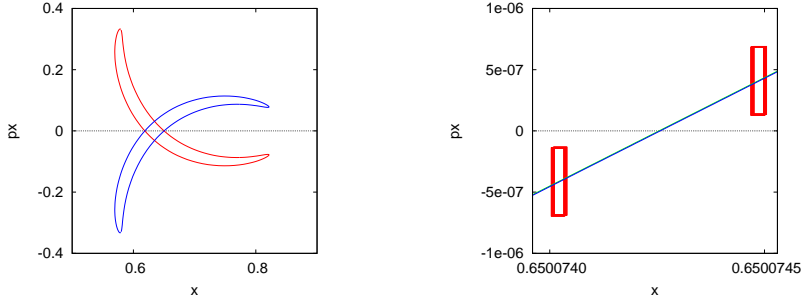


FIG. 7.6. *Left: Numerical sketch of $W^s(L(x))$ (in red) and $W^u(L(x))$ (in blue) intersected with $\{y = 0\}$. Right: we have proved that $\{\pi_{x,p_x}(W^u(L(x)) \cap \{y = 0\}) | x \in I\}$ consists of curves which pass through two red boxes. We have also proved that their slope is between $[1.7695, 1.7725]$. The blue/green line is a non-rigorous plot of the curves.*

We needed to subdivide B_E into 600 parts to compute $[DG(B_E)V^+]$ together with $[DG(B_E)V^-]$ with sufficient accuracy to obtain (7.16). Verification of assumptions of Lemma 7.8 took 24 minutes on a standard laptop.

REMARK 7.13. *From \mathbf{a} and by S -symmetry of manifolds $W^u(L(x))$ and $W^s(L(x))$, we obtain an estimate $[58.8637^\circ, 58.9439^\circ]$ on the angle of intersection of the curves on the x, p_x plane.*

REMARK 7.14. *At one go we obtain an estimate for a whole family of curves on*

$$\pi_{x,p_x}(W^u(L(x)) \cap \{y = 0\}) \quad \text{for } x \in I.$$

In reality these curves are very close to each other (at furthest distance along x of about $2.65 \cdot 10^{-9}$). We plotted (using non-rigorous computations) two curves which

are furthest from each other on the right hand side plot of Figure 7.6. One is in green and the other in blue. They are visible only after a large magnification, and on a paper printout will merge together. This means that our estimate on the position of the curves is somewhat rough in comparison to non-rigorous numerical simulation.

8. Closing Remarks and Future Work. In this paper we have presented a method for proving existence of families of Lyapunov orbits in the planar restricted circular three body problem. The method gives explicit bounds on a curve of initial points, which can continue up to half the distance from L_2 to the smaller primary in the Jupiter-Sun system.

We also presented a method of proving transversal intersections of invariant manifolds associated with Lyapunov orbits. The method gives explicit bounds on where the intersection takes place. It has been applied to Lyapunov orbits with energy of the comet Oterma in the Jupiter-Sun system.

In this paper we have focussed on detection of homoclinic intersections. Using identical tools one could also prove heteroclinic intersections of manifolds in the spirit of the work of Wilczak and Zgliczyński [19, 20].

Due to the fact that the presented method gives explicit estimates on the position of investigated manifolds, it is our hope to later apply it to the study of diffusion. Here is an outline of future scheme that could be followed to prove diffusion. The family of Lyapunov orbits is normally hyperbolic, hence survives time periodic perturbations. In non-autonomous setting the system no longer preserves energy, which allows for diffusion between orbits of different energies. Such mechanism has been investigated in [6] for the planar restricted elliptic three body problem, for the system with special restriction on parameters. The discussed diffusion follows from the geometric method of Delshams, de la Llave and Seara [8, 9, 10] and requires computation of Melnikov type integrals along homoclinic orbits of the PRC3BP. Since our method allows for precise and rigorous estimates for such orbits, it is our hope that such integrals could be computed using rigorous-computer assisted techniques. This combined with topological methods [5, 7] for detection of normally hyperbolic manifolds could give first rigorous results for diffusion in the three body problem with real life parameters. From this perspective, the results of this paper are a first step in a larger scheme for investigation of real life systems.

9. Acknowledgements. The author would like to thank Rafael de la Llave for discussions and remarks regarding implementation of the parameterization method. Special thanks go also to Daniel Wilczak for discussions on rigorous-computer-assisted computations using the CAPD library (<http://capd.ii.uj.edu.pl>).

10. Appendix.

10.1. Verification of Cone Conditions. LEMMA 10.1. *Let \mathbf{A} be an interval matrix of the form*

$$\mathbf{A} = \begin{pmatrix} \mathbf{a}_{11} & \varepsilon^T \\ \mathbf{B} & \mathbf{C} \end{pmatrix}$$

where $\mathbf{a}_{11} = [\underline{a}_{11}, \bar{a}_{11}]$ with $\underline{a}_{11} > 0$. If for any $\varepsilon \in \varepsilon$, $\|\varepsilon\| \leq \epsilon$ holds

$$\frac{\underline{a}_{11} - \epsilon\sqrt{\alpha}}{\sqrt{1 + \alpha}} > m, \quad (10.1)$$

then for $v = (x, y)$ such that $Q(v) = \alpha x^2 - \|y\|^2 \geq 0$ and any $A \in \mathbf{A}$ we have $\|Av\| > m \|v\|$.

Proof. For $v = (x, y)$ satisfying $Q(v) \geq 0$, we have $\|x\|^2 + \|y\|^2 \leq \|x\|^2 (1 + \alpha)$. Using (10.1) this gives the following estimate

$$\|Av\| \geq \underline{a}_{11} \|x\| - \epsilon \|y\| \geq (\underline{a}_{11} - \epsilon\sqrt{\alpha}) \|x\| > m\sqrt{\|x\|^2 + \|y\|^2} = m \|v\|.$$

□

LEMMA 10.2. *Let $Q(v) = Q(x, y) = \alpha x^2 - \|y\|^2$, let C_Q be a diagonal matrix such that $v^T C_Q v = Q(v)$, and let $\mathbf{A} = [DF(Q^+(v^*))]$. Assume that $\mathbf{D} = \mathbf{A}^T C_Q \mathbf{A}$ is an interval matrix of the form*

$$\mathbf{D} = \begin{pmatrix} \mathbf{d}_{11} & \boldsymbol{\varepsilon}^T \\ \boldsymbol{\varepsilon} & \mathbf{B} \end{pmatrix}.$$

Assume that $\mathbf{d}_{11} = [\underline{d}_{11}, \bar{d}_{11}]$ with $\underline{d}_{11} > 0$ and that for some $M > 0$, for any symmetric matrix $B \in \mathbf{B}$

$$\inf \{|\lambda| \mid \lambda \in \text{spec}(B)\} > -M. \quad (10.2)$$

If for any $\varepsilon \in \boldsymbol{\varepsilon}$ we have $\|\varepsilon\| \leq \epsilon$ and $\underline{d}_{11} - 2\epsilon > M\alpha$, then for any $v_1, v_2 \in U$, $v_1 \neq v_2$ such that $Q(v_1 - v_2) \geq 0$

$$Q(F(v_1) - F(v_2)) > 0.$$

Proof. By (6.9) $Q(F(v_1) - F(v_2)) = (v_1 - v_2)^T D (v_1 - v_2)$ for some symmetric matrix $D \in \mathbf{D}$.

For $v = (x, y)$ such that $Q(x, y) \geq 0$ and for any symmetric $D \in \mathbf{D}$

$$D = \begin{pmatrix} d_{11} & \varepsilon^T \\ \varepsilon & B \end{pmatrix}$$

we compute the following bounds

$$\begin{aligned} v^T Av &= d_{11}x^2 + x\varepsilon^T y + y^T \varepsilon x + y^T B y \\ &\geq \underline{d}_{11}x^2 - 2\epsilon \|y\| |x| - M \|y\|^2 \\ &\geq (\underline{d}_{11} - 2\epsilon)x^2 - M \|y\|^2 \\ &= M \left(\frac{\underline{d}_{11} - 2\epsilon}{M} x^2 - \|y\|^2 \right) \\ &> MQ(x, y) \\ &> 0. \end{aligned}$$

□

REMARK 10.3. *Assumption (10.2) is easily verifiable from Gershgorin theorem.*

10.2. Bounds for the Images in Local Coordinates . Here we give a proof of Lemma 7.3.

Proof. Inclusion (7.6) is equivalent to showing that for any $\tau \in \mathbf{T}$, and any $v_1 \in U_1$ there exists an v_2 in U_2 such that

$$G(\tau, v_1, v_2) = 0. \quad (10.3)$$

Let us fix a $\tau \in \mathbf{T}$ and $v_1 \in U_1$ and use a notation $G_{\tau, v_1}(v_2) = G(\tau, v_1, v_2)$. Observe that $[DG_{\tau, v_1}(U_2)] \subset \mathbf{A}(U_2)$ and $[G_{\tau, v_1}(v_0)] \subset [G(\mathbf{T}, U_1, v_0)]$. Since from (7.5)

$$v_0 - [DG_{\tau, v_1}(U_2)]^{-1} G_{\tau, v_1}(v_0) \subset N(\mathbf{T}, v_0, U_1, U_2) \subset U_2,$$

by the interval Newton method (Theorem 2.1) there exists a unique $v_2 = v_2(\tau, v_1) \in U_2$, which satisfies (10.3). \square

REMARK 10.4. *When applying Lemma 7.3, due to very strong hyperbolicity of the map Φ_τ it pays off to use the mean value theorem. Taking $U_1 = v_1 + B$ we can compute*

$$N(\mathbf{T}, v_0, U_1, U_2) = v_0 - [\mathbf{A}(U_2)]^{-1} G(\mathbf{T}, v_1, v_0) - \left[\left(\mathbf{A}(U_2)^{-1} \frac{\partial G}{\partial v_1}(\mathbf{T}, U_1, v_0) \right) B \right].$$

This is a better form since in (below we neglect arguments in order to keep the formula compact)

$$\mathbf{A}^{-1} \frac{\partial G}{\partial v_1} = -D\lambda^{-1} \cdot \left((D\psi)^{-1} \cdot D\tilde{\Phi}_\tau \cdot D\psi \right), \quad (10.4)$$

the strong hyperbolic expansion cancels out. This is the main advantage of Lemma 7.3.

Here we give a technical lemma that can be used for computation of

$$\psi^{-1}(C^{-1}((x, 0, 0, \kappa(x)) - q^0)) \quad \text{for } x \in I$$

and $q^0 = (x^0, 0, 0, p_y^0)$. Below, R can be any matrix close to $D\psi^{-1}(0)C^{-1}A$.

LEMMA 10.5. *Let $a \in \mathbb{R}$ and $J_1 \subset \mathbb{R}$ be from Lemma 3.1 and let*

$$A = \begin{pmatrix} 1 & 0 & 0 & 0 \\ 0 & 1 & 0 & 0 \\ 0 & 0 & 1 & 0 \\ a & 0 & 0 & 1 \end{pmatrix}.$$

Let \mathbf{B} be a set in \mathbb{R}^4 , let R be a 4×4 matrix and let

$$M := [A^{-1}PD\psi(RB)R]^{-1}(I - x^0, 0, 0, J_1 - p_y^0).$$

If

$$M \subset \mathbf{B} \quad (10.5)$$

then $\psi^{-1}(C^{-1}((x, 0, 0, \kappa(x)) - q^0)) \subset RB$.

Proof. By Lemma 3.1

$$\begin{aligned} (x, 0, 0, \kappa(x)) &\in (x^0, 0, 0, p_y^0) + (I - x^0, 0, 0, a(I - x^0) + J_1 - p_y^0) \\ &= q^0 + A(I - x^0, 0, 0, J_1 - p_y^0), \end{aligned}$$

hence

$$(x, 0, 0, \kappa(x)) - q^0 \in A(I - x^0, 0, 0, J_1 - p_y^0). \quad (10.6)$$

Let

$$G_q(p) = A^{-1}C\psi(Rp) - q$$

If we can show that for any $q \in (I - x^0, 0, 0, J_1 - p_y^0)$ there exists a $p \in \mathbf{B}$ such that

$$G_q(p) = 0 \quad (10.7)$$

then

$$\psi^{-1}(C^{-1}Aq) = Rp,$$

hence by (10.6)

$$\psi^{-1}(C^{-1}((x, 0, 0, \kappa(x)) - q^0)) \subset R\mathbf{B}.$$

To show (10.7) we apply the interval Newton method (Theorem 2.1). Since $\psi(0) = 0$ we can compute

$$\begin{aligned} N(0, \mathbf{B}) &= - \left[\frac{d}{dp} G_q(\mathbf{B}) \right]^{-1} G_q(0) \\ &= - [A^{-1}CD\psi(R\mathbf{B})R]^{-1} (-q) \\ &\subset M, \end{aligned}$$

and by (10.5) combined with Theorem 2.1 obtain (10.7), and hence obtain our claim.

□

REFERENCES

- [1] R. Abraham, J. Marsden, *Foundations of mechanics*. Benjamin/Cummings Publishing Co., Inc., Advanced Book Program, Reading, Mass. (1978).
- [2] G. Alefeld, *Inclusion methods for systems of nonlinear equations - the interval Newton method and modifications*. Topics in validated computations (Oldenburg, 1993), 7–26, Stud. Comput. Math., 5, North-Holland, Amsterdam, 1994.
- [3] R. Broucke. *Periodic orbits in the restricted three-body problem with Earth-Moon masses*. NASA-JPL technical report 32-1168 (1968), available at: ntrs.nasa.gov/archive/nasa/casi.ntrs.nasa.gov/19680013800_1968013800.pdf.
- [4] X. Cabré, E. Fontich, R. de la Llave, *The parameterization method for invariant manifolds. III. Overview and applications*. J. Differential Equations 218 (2005), no. 2, 444–515.
- [5] M. J. Capiński, P. Roldán, *Existence of a Center Manifold in a Practical Domain around L_1 in the Restricted Three Body Problem*, to appear in SIADS.
- [6] M. J. Capiński and Piotr Zgliczyński. *Transition tori in the planar restricted elliptic three-body problem* Nonlinearity, 24:1395–1432, 2011.
- [7] M. J. Capiński and Piotr Zgliczyński. *Cone conditions and covering relations for topologically normally hyperbolic manifolds*. Discrete Contin. Dyn. Syst., 30(3):641–670, 2011.
- [8] A. Delshams, R. de la Llave, T. Seara, *A geometric approach to the existence of orbits with unbounded energy in generic periodic perturbations by a potential of generic geodesic flows of T^2* . Comm. Math. Phys. 209 (2000), no. 2, 353–392.
- [9] A. Delshams, D. de la Llave, T. Seara, *A geometric mechanism for diffusion in Hamiltonian systems overcoming the large gap problem: heuristics and rigorous verification on a model*. Mem. Amer. Math. Soc. 179 (2006), no. 844,
- [10] A. Delshams, D. de la Llave, T. Seara, *Geometric properties of the scattering map of a normally hyperbolic invariant manifold*. Adv. Math. 217 (2008), no. 3, 1096–1153.
- [11] G. Gómez, À. Jorba, C. Simó, and J. Masdemont. *Dynamics and mission design near libration points. Vol. III*, volume 4 of *World Scientific Monograph Series in Mathematics*. World Scientific Publishing Co. Inc., River Edge, NJ, 2001. Advanced methods for collinear points.
- [12] G. Gómez, W. S. Koon, M. W. Lo, J. E. Marsden, J. Masdemont, and S. D. Ross. *Connecting orbits and invariant manifolds in the spatial restricted three-body problem*. Nonlinearity, 17(5):1571–1606, 2004.
- [13] À. Jorba and C. Simó. *Effective stability for periodically perturbed Hamiltonian systems in Hamiltonian mechanics* (Toruń, 1993), volume 331 of NATO Adv. Sci. Inst. Ser. B Phys., pages 245–252. Plenum, New York, 1994.

- [14] À. Jorba and J. Villanueva. *Numerical computation of normal forms around some periodic orbits of the restricted three-body problem*. Phys. D, 114(3-4):197–229, 1998.
- [15] W. Koon, M. Lo, J. Marsden and S. Ross, *Heteroclinic connections between periodic orbits and resonance transitions in celestial mechanics* Chaos 10 (2000), 42769
- [16] J. Llibre, R. Martinez, C. Simó, *Transversality of the Invariant Manifolds Associated to the Lyapunov Family of Periodic Orbits Near L_2 in the Restricted Three Body Problem*, Journal of Differential Equations 58 (1985), 104-156.
- [17] Jürgen Moser. *On the generalization of a theorem of A. Liapounoff*. Comm. Pure Appl. Math., 11:257–271, 1958.
- [18] C. L. Siegel and J. K. Moser. *Lectures on celestial mechanics*. Classics in Mathematics. Springer-Verlag, Berlin, 1995. Translated from the German by C. I. Kalme, Reprint of the 1971 translation.
- [19] D. Wilczak, P. Zgliczyński, *Heteroclinic Connections between Periodic Orbits in Planar Restricted Circular Three Body Problem - A Computer Assisted Proof*, Comm. Math. Phys. 234 (2003) 1, 37-75,
- [20] D. Wilczak, P. Zgliczyński, *Heteroclinic Connections between Periodic Orbits in Planar Restricted Circular Three Body Problem - Part II* , Comm. Math. Phys. 259, 561-576 (2005),
- [21] P. Zgliczyński, *Covering relations, cone conditions and the stable manifold theorem*. J. Differential Equations 246 (2009), no. 5, 1774–1819.